DIFFERENTIAL EQUATION BASED LENGTH SCALE EVALUATIONS FOR DES, RANS AND MOVING GRID SOLUTIONS

Paul G. Tucker
Fluid Dynamics Research Centre
University of Warwick, Coventry CV4 7AL
P.Tucker@warwick.ac.uk

ABSTRACT

Surprisingly expensive to compute wall distances are still used in a range of key turbulence models. Potentially economical, accuracy improving differential equation based distance algorithms are described. These involve an elliptic Poisson and a hyperbolic natured Eikonal equation approach. Eikonal extension to a Hamilton-Jacob equation is discussed. Use of this to improve turbulence model accuracy and, along with the Eikonal, enhance Detached Eddy Simulation (DES) techniques is considered. Although less accurate than the Eikonal, Poisson method based flow solutions are extremely close to those using a search procedure. For a moving grid case the Poisson method is found especially efficient. Results show that with care the Eikonal equation can be solved on highly stretched, non-orthogonal, curvilinear grids.

INTRODUCTION

Wall distances, d, are still a primary parameter in a range of key turbulence models (Fares and Schroder, 2002). Surprisingly, for highly optimised RANS/URANS (Unsteady Reynolds Averaged Navier-Stokes) solvers, the effort in calculating d can be a significant fraction of the total solution time. For example, even with Cray C90 class computers it can take 3 hours just to gain d (Wigton, 1998). For flows with time dependent geometry (such as Computational Aeroelasticity) or mesh refinement clearly this feature is exacerbated (Boger, 2001).

Because of d evaluation expense in some codes dangerous approximations are made (Spalart, 2000). These will give mostly unhelpful inexact distances $\tilde{d}$. However, the careful modification of d to some $\tilde{d}$ can remedy turbulence model deficiencies or extend modelling potential (Fares and Schroder, 2002). For example, if $\tilde{d} = d$ sharp convex features such as a thin wire (referred to here as the *'thin wire problem'*) or wing trailing edge can have disproportionate turbulence influences. Wall proximity reduces eddy viscosity through boosting turbulence destruction terms. Hence, the excessive influence of sharp convex features can be lessened by ensuring $\tilde{d} > d$. For corners or bodies/surfaces in close proximity the increased multiple surface turbulence damping effect (Mompean et al., 1996) should be taken into account. Setting $\tilde{d} < d$ is a convenient mechanism for achieving this. Relative to search procedures differential equation based methods offer the possibility of both efficiency and accuracy gains. Differential equation wall distance methods are now discussed.

Differential equation based distance methods

Poisson equation method. A Poisson equation (Tucker, 2000) d method proposed by Spalding can be used. For this, the equation

$$\nabla^2\phi = -1 \tag{1}$$

is solved inside the flow domain Ω with boundaries $\tilde{\Gamma}$. Gradients of ϕ are used to gain d. For curved surfaces the following near wall accurate L_2 norm based approximation is recommended

$$d = \pm\sqrt{\sum_{j=1,3}\left(\frac{\partial\phi}{\partial x_j}\right)^2} + \sqrt{\sum_{j=1,3}\left(\frac{\partial\phi}{\partial x_j}\right)^2 + 2\phi} \tag{2}$$

Eikonal equation method. To directly gain d, Sethain (1999) proposes the following hyperbolically behaved Eikonal equation

$$|\nabla\phi| = 1 \tag{3}$$

where $\phi = t$ – the first *arrival time* of a propagating front. The right hand side of unity characterises the front propagation velocity. For this unit velocity $d = t$. Here a Laplacian is deliberately added to (3) to give the following Hamilton-Jacobi (HJ) equation

$$|\nabla\phi| = 1 + \Gamma\nabla^2\phi \tag{4}$$

The Laplacian allows control of the front propagation velocity, U, to gain $\tilde{d}$. The U can now be considered equal to $(1+\Gamma\nabla^2\phi)^{-1}$. Eikonal equation solution in non-orthogonal coordinates is uncertain (Sethain, 2002). Hence, this aspect is also considered in the present work.

Laplacian form and role. Near a fine convex feature (wire) for theoretical correctness accurate distances are needed so $\tilde{d} = d$. However, to prevent excessive far field influence $\tilde{d} >> d$. Since adjacent to a convex feature $\Gamma\nabla^2 d >> 0$, with Laplacian inclusion the desired effect of exaggerating d (i.e. delaying first arrival times) is naturally gained. Motivated by dimensional homogeneity, the need that as $d \to 0$, $\tilde{d} = d$ but $\nabla^2\phi \to \infty$ suggests

$$\Gamma = \varepsilon d \qquad (5)$$

where ε is a constant. Clearly more 'aggressive' functions than (5) (e.g. $\Gamma = \varepsilon(-1 + e^{d})$) are possible but these are not explored.

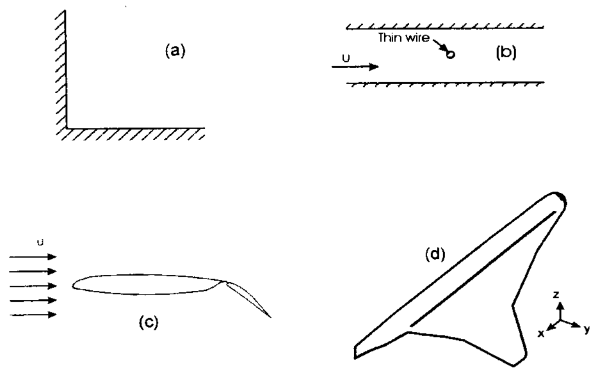

Figure. 1. Geometries considered: (a) Corner region; (b) plane channel with thin wire; (c) wing and flap and (d) double-delta configuration.

At corners $\nabla^2 d < 0$, hence $\tilde{d} << d$. Therefore, with the Laplacian, the damping effects of 'extra' walls, discussed earlier, is naturally accounted for. The Laplacian also has the potential to lessen non-smoothness issues (Strelets, 2001) associated with SA (Spalart and Allmaras, 1994) DES.

NUMERICAL METHOD

Following Sethian for 'inviscid terms' the 1st order scheme due to Godunov is used

$$|\nabla\phi| \approx \begin{Bmatrix} \max(\Delta_{i-1,j,k}\phi, -\Delta_{i+1,j,k}\phi, 0)^2 + \\ \max(\Delta_{i,j-1,k}\phi, -\Delta_{i,j+1,k}\phi, 0)^2 + \\ \max(\Delta_{i,j,k-1}\phi, -\Delta_{i,j,k+1}\phi, 0)^2 \end{Bmatrix}^{1/2} = RHS_{i,j,k} \qquad (6)$$

Assuming a transformed (ξ, η, ς) system

$$\Delta_{i-1,j,k}\phi = \frac{\phi_i - \phi_{i-1}}{\Delta\xi}, \quad \Delta_{i+1,j,k}\phi = \frac{\phi_{i+1} - \phi_i}{\Delta\xi} \qquad (7)$$

The subscripts refer to grid point locations. Equation (6) ignores non-orthogonal terms. These must be treated in a manner consistent with (6). When the right hand side of (6) ($RHS_{i,j,k}$) involves diffusion terms or the Poisson equation is being solved, standard second order central differencing is used. As results will show, the differences used in the transformed Eikonal equation Jacobian terms need to be treated with care. Central differences can be used or differences upwinded in the propagating front direction.

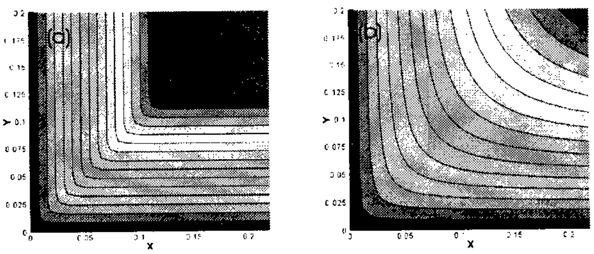

Figure. 2. Influence of Laplacian on d at corners: (a) Eikonal solution and (b) HJ solution.

Starting conditions. For SA DES when using the Eikonal equation, the following starting condition (initial guess) is sufficient

$$\phi = C_{DES}\Delta_i \ \text{ in } \Omega \qquad (8)$$

where C_{DES} is a modelling constant. The d computation will naturally terminate when, at the active front, $d \geq C_{DES}\Delta_i$. For most DES implementations d is needlessly evaluated for all Ω. With the current approach this wasted computational effort is avoided. Also, the d array is such that, if read into a sufficiently accurate URANS solver, with the SA model activated, a DES solution will naturally arise. No code modifications or needless intrinsic arguments are needed. For Eikonal based RANS, zonal RANS and the zonal LES of Tucker and Davidson (2003) the starting condition below can be used

$$\phi = d_{max} \ \text{ in } \Omega \qquad (9)$$

With zonal RANS/LES d_{max} could correspond to a prescribed model interface. For RANS economy, d_{max} could characterise the near wall turbulence destruction term activity range. Here, for internal flows without zonal modelling $d_{max} \to \infty$ is used. This is a safe default value. For Poisson method predictions $\phi = 0$ in Ω is adequate.

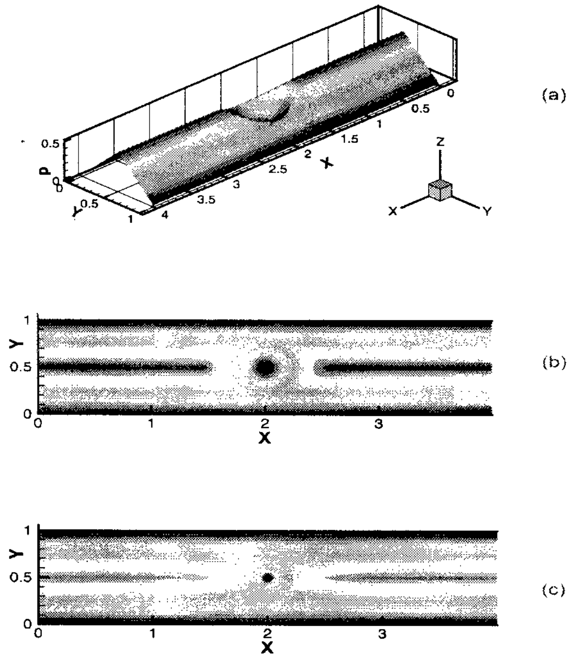

Figure 3. Eikonal and HJ solutions: (a) 3D Eikonal solution view; (b) 2D Eikonal solution view and (c) 2D HJ view

Boundary conditions. At smooth solid walls the following Dirichlet condition is applied

$$\phi = 0 \text{ on } \tilde{\Gamma} \tag{10}$$

At flow/far field boundaries

$$\frac{\partial \phi}{\partial n} = 0 \text{ on } \tilde{\Gamma} \tag{11}$$

can be used, where n is the boundary normal co-ordinate. However, if Ω is sufficiently large, (10) makes a stable far field condition. This is used here for the Poisson method.

Eikonal based equations are tested for overset and abutted grids. For the abutted, on non-solid surface block boundaries differential conditions (Equation (11)) are, due to the interface nature, found adequate. For the overset, a mono-block grid Eikonal solution is represented on a dual block flow solution grid. The above two approaches avoid generating two quite different multi-block Eikonal solvers.

General solution information. When evaluating Equation (2), away from solid walls second order central differences are used. For simplicity, with multiblock solutions at block boundaries first order backward differences are implemented. The Poisson method simultaneous equations are solved using a crude ADI procedure. The Eikonal equation is solved using a propagating front method (see Sethian, 1999). When solving the HJ equation, an Eikonal solution is used as an initial guess and then a Newton solver applied. Modified versions of two structured grid, flow solvers are used. These are the NASA CFL3D (Rumsey et al., 1996) and NTS (Shur et al., 1999) codes.

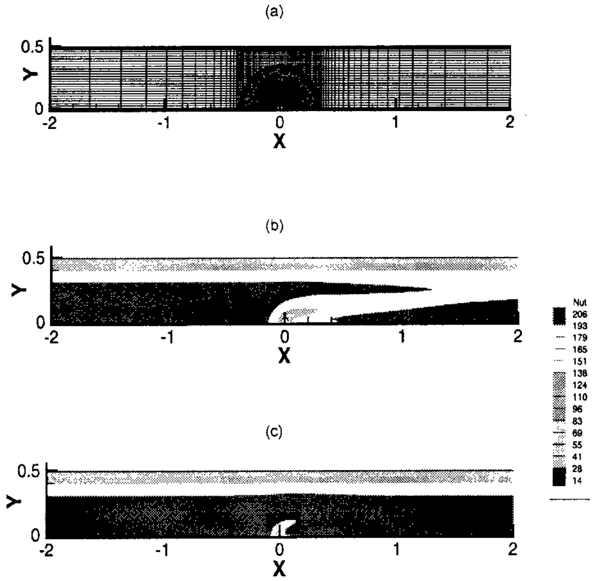

Figure 4. Grid and turbulent viscosity contours: (a) grid; (b) Eikonal contours and (c) HJ contours

DISCUSSION OF RESULTS

The following Figure 1 geometries are considered: (a) Corner region; (b) Plane channel with a thin wire; (c) Wing with flap and (d) Double delta wing configuration.

Corner Region (Case (a)). Figure 2, frames (a) and (b) give Eikonal and HJ d solutions, respectively. Frame (b) shows the latter correctly (see DNS data of Mompean et al., 1996) allows the turbulence model to sense the damping influence of both corner walls.

Plane channel flow with wire (Case (b)). The 'thin wire problem' is explored using an SA model solution for a fully developed plane channel flow with a wire (see Figure 1b) and $Re = 1\text{x}10^5$. The wire diameter is 1/40th the channel width. Figure 3 gives representations of the pure Eikonal and HJ equation distances. Frame (a) is a 3D (three-dimensional) representation of the pure Eikonal solution. Frames (b) and (c) are 2D plots of pure Eikonal and HJ solutions, respectively. The desired 'vanishing' effect of the Laplacian on the wire is evident. Figure 4 gives the over-set flow solution grid and also turbulent viscosity contours. The Figure 4, frames (b) and (c) give turbulent viscosity contours for solutions with and without the Laplacian distance modification. The Laplacian based modification has helped with the excessive wire influence but caution is required since ε must not be too large.

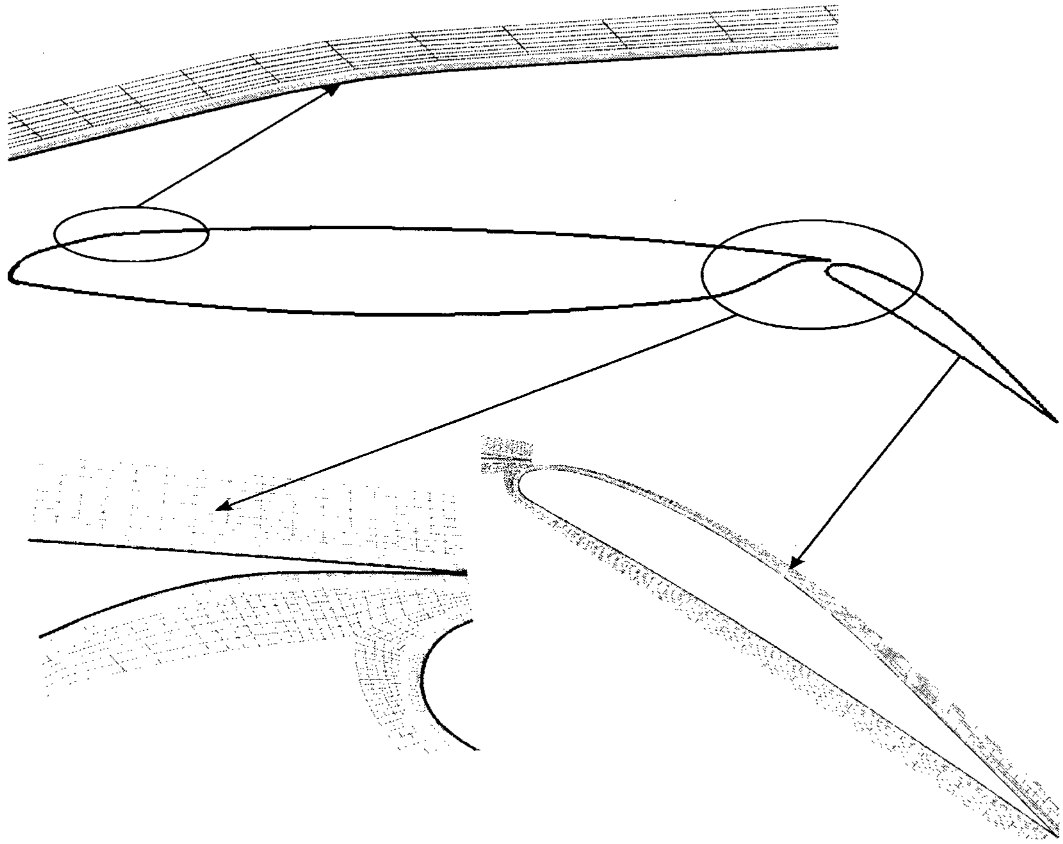

Figure 5. Eikonal equation wall distance coloured grid features for wing-flap configuration.

Wing with flap (Case (c)). In a zonal LES (Tucker and Davidson, 2003) context (for y^+<250), Figure 5 shows Case (c) Eikonal d coloured grid features. As typical for high-speed flows, the grid is highly stretched in the wall normal direction. Figure 6 shows top wing surface, mid-chord, Eikonal d results plotted against normal wall distance. The frame (a) and (b) vertical axes are d and % error, respectively. As can be seen, for highly stretched grids, using upwind based metric differences that are consistent with the main discretization improves accuracy. Frame (a) shows, without metric upwinding the d error grows (i.e. is additive) with surface distance.

The Eikonal and Poisson equation methods have average d errors of 0.8 and 0.97 %, respectively. Figure 7 gives $y^+ < 400$ error histograms for the Eikonal (with cross-derivatives) and Poisson based approaches. Negative errors correspond to d over predictions. For both methods, conveniently, errors increase away from walls, where, for turbulence models, they matter less. Clearly, the Frame (a) Eikonal equation error distribution is most symmetrical. For the Poisson method (see Frame (b)), there is a d over-prediction trait. This is partly due to relatively fine convex features (the Poisson method tends to over-predict d in such regions which is beneficial) and also because grid orthogonality has been assumed.

As noted earlier, for this case, the Poisson method is less accurate than the Eikonal. However, SA model Poisson method lift and drag coefficients are within 0.05% of those for the search procedure. These values being for a solution with Re = 23 x 10^6, based on the wing chord and a Mach number, Ma = 0.18. Around 1 million cells give sensibly grid independent solutions.

Double delta wing (Case (d)). Figure 8 gives the Case (d) Poisson method d error histogram. For this more complex configuration the average error is higher at 2.67 %. The Eikonal equation is not considered for this case.

A key Case (d) motivation is aeroelasticity studies. For details of the CFL3D mesh deformation approach, that freshly initialises the d search procedure for each moving mesh time-step, see Bartels (2000). Figure 9 shows initial and severely deformed aeroelasticity calculation surface meshes. For moving mesh performance studies ten approximately equi-spaced deflection increments between the Figure 9 extremes are considered. These large increments and the strongly deformed Figure 9b grid are intended to give poor cell types that most severely test the Poisson method. The search procedure takes around 20% of the time step cost and the Poisson method cost is found to be $1/6^{th}$ that for the search. Even, for the far more challenging fixed mesh case the Poisson method is found considerably faster than the search.

Encouragingly, the Case (d), CFL3D, SA model based lift and drag coefficients for the Poisson method are within 0.03 and 0.06 % of those for the search procedure. These values being for $Re = 2.2\times10^6$ (based on the half wing span), $Ma = 0.96$ and a modest circa 1 million cell grid.

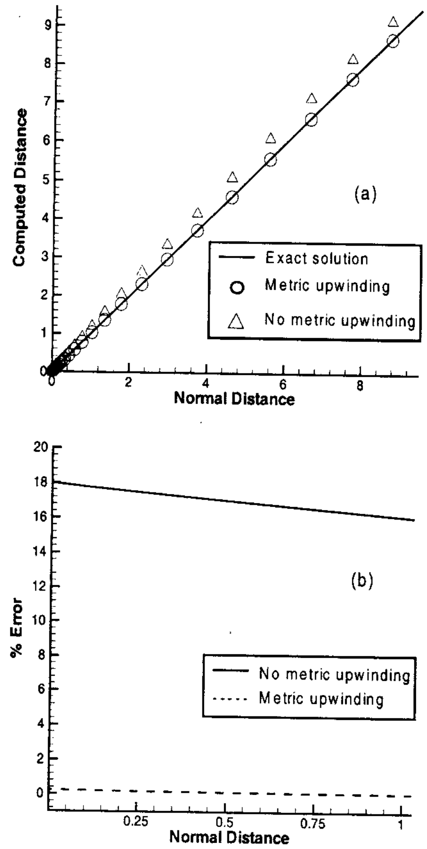

Figure 6. Eikonal equation errors for solutions with an without Jacobian upwinding: (a) Computed d and (b) Error in d.

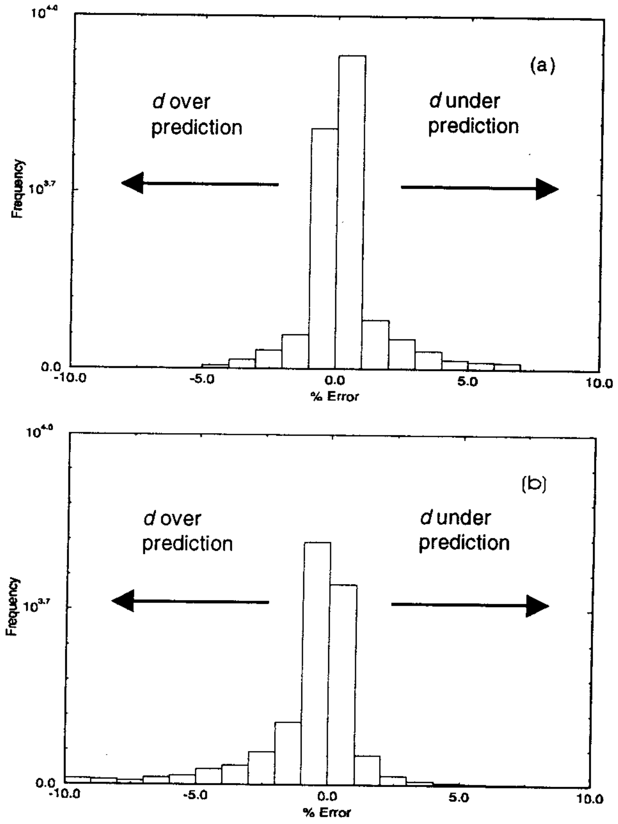

Figure 7. Case (c) d error histogram: (a) Eikonal method and (b) Poisson method.

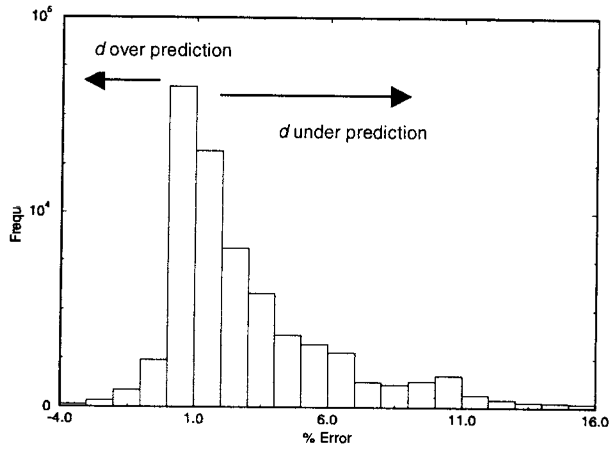

Figure 8. Case (d) d error histogram for Poisson method.

CONCLUSIONS

The Poisson method distance algorithm is around twice as fast as the search procedure. With parallel and vector processing this could be improved. Although less accurate than the Eikonal, Poisson method based flow solutions are extremely close to those using a search procedure. For moving grids that do not preserve grid topology the Poisson method is much faster than the search procedure. It is possible to solve the Eikonal equation on highly stretched non-orthogonal curvilinear grids. However, this hyperbolic natured equation is not straightforward to economically solve and can display instability. For accuracy, Eikonal metrics must be upwinded in the front propagation direction. Addition of a distance scaled Laplacian to the Eikonal equation gives beneficial wall distance properties that can reduce the 'thin wire problem'.

ACKNOWLEDGEMENTS

The present work was carried out at Boeing Commercial Aeroplanes, Seattle amid a group of exceptionally kind people. It was mostly funded through a Royal Academy of Engineering Secondment Award. I am very grateful for this award and to P. R. Spalart for making the visit possible and his very generous encouragement and support during the visit. I would like to thank, L. Hedges, M. Hong, C. Rumsey, J. Sethain, M. Shur, M. Strelets, L. Wigton, and V. Venkatakrishnan for their kind help. Especial thanks are due to C. Hilmes. Other members of

Boeing staff have also been very helpful and I apologise if I have forgot to acknowledge you.

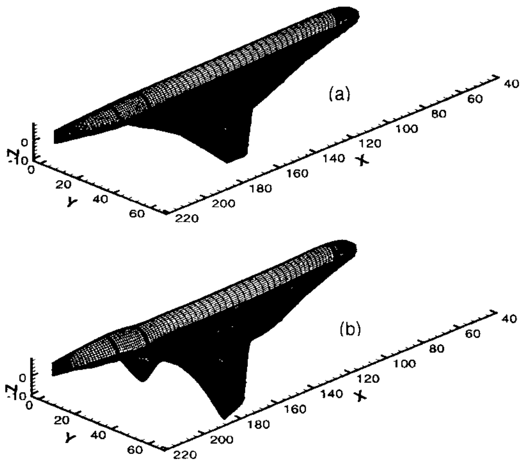

Figure 9. Initial and fully deformed Case (d) surface meshes.

REFERENCES

Bartels, R. E, 2000, "Mesh strategies for accurate computation of unsteady spoiler and aeroelastic problems," *J. of Aircraft*, Vol. 37, No. 3, pp. 521-525.

Boger, D. A, 2001, "Efficient method for calculating wall proximity," *AIAA Journal*, Vol. 39, No. 12, pp. 2404-2406 (2001)

Fares, E., and Schroder, W., 2002, "A differential equation to determine the wall distance," *Int. J. for Num. Meths in Fluids*, Vol. 39, pp 743-762.

Mompean, G., Gavrilakis, S., Machiels, L., and Deville, M., O., 1996, "On predicting the turbulence-induced secondary flows using non-linear k-ε models," *Phys. Fluids*, Vol. 8, No. 7, pp. 1856-1868.

Rumsey, L., Sanetrix, M. D., Biedron, R. T., Melson, N. D. and Parlette, E. B., 1996, "Efficiency and accuracy of time-accurate turbulent Navier-Stokes computations," *Computers and Fluids*, Vol. 25, No. 2, 1996, pp.217-236 (1996)

J. A. Sethian, "Fast Marching Methods," *SIAM Review*, Vol. 41, No. 2, 199-235.

Sethian, J. A., 2002, Personal communication.

Shur, M., Spalart, P. R., Strelets, M. and Travin, A., 1999, "Detached-eddy simulation of an aerofoil at high angle of attack," *Proc. 4th Int. Symp. on Engineering Turbulence Modelling and Measurements, Ajaccio, Corsica, France*, pp. 669-678.

Spalart, P. R., and Allmaras, S. R., 1994, "A one-equation turbulence model for aerodynamic flows," *La Rech. Aerospatiale*, Vol. 1, pp. 5-21.

Strelets, M., 2001, "Detached eddy simulation of massively separated flows," *AIAA Paper* 2001-0879.

Tucker, P. G., 2000, "Prediction of turbulent oscillatory flows in complex systems," *Int. J. for Num. Meths in Fluids*, Vol. 33, pp. 869-895.

Tucker, P. G. and Davidson, L., 2003, "Zonal k-l based large eddy simulations," *AIAA Paper* 2003-0082.

Wigton, L. B., 1998, "Optimizing CFD codes and algorithms for use on Cray computers," *Frontiers of Computational Fluid Dynamics (Editors D. A. Caughey and M. M. Hafez), Chapter 16, pp. 1-15, World Scientific Publishing Co. Pte. Ltd.*